the FEBS Journal

The hinge region operates as a stability switch in cGMP-dependent protein kinase Iα

Arjen Scholten[1,2], Hendrik Fuß[1,*], Albert J. R. Heck[2] and Wolfgang R. Dostmann[1]

1 Department of Pharmacology, College of Medicine, University of Vermont, Burlington, VT, USA
2 Department of Biomolecular Mass Spectrometry, Bijvoet Center for Biomolecular Research and Utrecht Institute for Pharmaceutical Sciences, Utrecht University, the Netherlands

Keywords
cGMP; cGMP-dependent protein kinase Iα; limited proteolysis; mass spectrometry; tryptophan fluorescence

Correspondence
W. R. Dostmann, Department of Pharmacology, College of Medicine, University of Vermont, 149 Beaumont Avenue, Burlington, VT 05405, USA
Fax: +1 802 6564523
Tel: +1 802 6560381
E-mail: wolfgang.dostmann@uvm.edu

***Present address**
University of Ulster, School of Biomedical Sciences, Cromore Road, Coleraine, BT52 1SA, UK

(Received 19 September 2006, revised 28 January 2007, accepted 1 March 2007)

doi:10.1111/j.1742-4658.2007.05764.x

The molecular mechanism of cGMP-dependent protein kinase activation by its allosteric regulator cyclic-3′,5′-guanosine monophosphate (cGMP) has been intensely studied. However, the structural as well as thermodynamic changes upon binding of cGMP to type I cGMP-dependent protein kinase are not fully understood. Here we report a cGMP-induced shift of Gibbs free enthalpy ($\Delta\Delta G_D$) of 2.5 kJ·mol^{-1} as determined from changes in tryptophan fluorescence using urea-induced unfolding for bovine PKG Iα. However, this apparent increase in overall stability specifically excluded the N-terminal region of the kinase. Analyses of tryptic cleavage patterns using liquid chromatography-coupled ESI-TOF mass spectrometry and SDS/PAGE revealed that cGMP binding destabilizes the N-terminus at the hinge region, centered around residue 77, while the C-terminus was protected from degradation. Furthermore, two recombinantly expressed mutants: the deletion fragment Δ1-77 and the trypsin resistant mutant Arg77Leu (R77L) revealed that the labile nature of the N-terminus is primarily associated with the hinge region. The R77L mutation not only stabilized the N-terminus but extended a stabilizing effect on the remaining domains of the enzyme as well. These findings support the concept that the hinge region of PKG acts as a stability switch.

The cGMP-dependent protein kinase Iα (PKG) is a major branch point in the nitric oxide and natriuretic peptide-induced cGMP-signaling pathway. PKG plays a pivotal role in several important biological processes such as the regulation of smooth muscle relaxation [1] and synaptic plasticity [2]. Consequently, several substrates for PKG are established in smooth muscle, cerebellum and platelets (for review, see [3]).

The holoenzyme of PKG is a noncovalent dimer composed of two identical subunits of ~76 kDa. Each PKG monomer harbors several different functional domains associated with their respective N-terminal, regulatory and C-terminal, catalytic subdomains. The regulatory domain contains a dimerization site, an auto-inhibitory motif and several autophosphorylation sites that have an effect on basal kinase activity, i.e. in the absence of cGMP [4] and cyclic nucleotide binding kinetics [5,6]. In addition, it has been proposed that autophosphorylation of PKG induces a conformational change comparable to binding of cGMP to the regulatory domain [7]. The N-terminus of the protein is also responsible for the intracellular localization [8–10]. A hinge region connects the N-terminal dimerization site with the two in-tandem cGMP binding pockets and it has been postulated that its function is to serve as the enzyme's auto-inhibitory site [11–13].

Abbreviations
MEW, maximal emission wavelength; PKA, cAMP-dependent protein kinase; PKG, cGMP-dependent protein kinase Iα.

The two in-tandem cGMP binding pockets of PKG have different binding characteristics [14]; the N-terminal high affinity site and the succeeding low affinity site display slow and fast cGMP-exchange characteristics and affinity constants of 17 and 100–150 nM, respectively [5,15]. Binding of cGMP to these sites activates the enzyme and shows positive cooperative behavior, which is abolished upon autophosphorylation of the enzyme [5]. The C-terminal part of the protein contains the catalytic domain, which consists of a Mg/ATP binding pocket and a substrate binding site.

In vitro studies have demonstrated that PKG is quite labile and susceptible to proteolytic digestion, particularly in the N-terminal domain [16–18]. Dimeric PKG is rapidly cleaved by trypsin, resulting in two C-terminal, monomeric fragments of ~67 kDa and a dimeric N-terminal fragment of ~18 kDa [16]. In PKG Iα, trypsin cleaves preferentially at arginine77 (R77) of the hinge region, thereby eliminating the dimerization and auto-inhibitory domains [19]. Interestingly, the resulting monomeric fragment (Δ1-77) retains similar catalytic properties (K_m, V_{max}) to wild-type PKG [17]. Although monomeric, PKG Δ1-77 can still bind two cGMP molecules (with similar overall K_d), the fragment is constitutively active and thus does no longer require binding of cGMP [17,18]. Also, in PKG Δ1-77 the cooperative nature of cGMP binding is lost [4,17]. So far, no biological function has been attributed to this monomeric, active form of PKG *in vivo*.

In full-length wild-type PKG Iα, cGMP binding is essential for full activity, however, the kinase also shows basal activity in absence of cGMP. It is believed that cGMP binding induces an elongation of the protein [20,21]. FT-IR data suggest that the conformational change induced by cGMP binding is primarily due to a topographical movement of the structural domains of PKG rather than to secondary structural changes within one or more of the individual domains [21]. The conformational change induced by cGMP binding is thought to induce the release of the auto-inhibitory domain from the active site, thereby activating the kinase. This is indicated by a remarkable increase in the proteolytic sensitivity of the N-terminus in the presence of cGMP, indicating that a conformational change has occurred that increases the solvent exposure of this region [22].

Crystal structures of a similar enzyme from the AGC-family of protein kinases, cAMP-dependent protein kinase (PKA) have greatly contributed to our understanding of PKG's intra- and inter-domain interactions, particularly the recent structure of the PKA holoenzyme [23]. Many biophysical techniques have been amended to obtain functional and structural data on PKG, however, to date, it has not been possible to obtain a high resolution crystal structure of PKG. The only PKG-specific structural information, by NMR, is limited to the very N-terminal dimerization part of the kinase [24]. Therefore, it is difficult to fully understand the different domain interactions in presence and absence of cGMP. The interaction of the auto-inhibitory domain with the catalytic domain in the presence and absence of cGMP is of particular interest, as it forms the centre of PKG's activation mechanism.

In this study, we provide new insights into the effect of cGMP binding on the domain stability of bovine cGMP-dependent protein kinase Iα (PKG). Therefore, apart from wild-type PKG, two mutants were recombinantly expressed: Δ1-77 and R77L, with the latter potentially leading to a more stable enzyme. More precisely, by using limited proteolysis in combination with mass spectrometry and urea unfolding assays we explored how the domain stability of these three different PKG forms is affected by cGMP binding.

Results

Tryptophan fluorescence monitoring in presence and absence of cGMP

The characterization of cGMP binding to PKG reported thus far provides little information regarding changes in the stability of the enzyme. Thus, we first employed intrinsic tryptophan fluorescence to probe large domain movements and changes in PKG's overall architecture with regard to cGMP binding. To elucidate whether cGMP can induce stability in the structure of PKG, the intrinsic fluorescence of PKG's eight tryptophan residues was probed in the presence and absence of cGMP. Figure 1A,B shows the intrinsic fluorescence emission spectra of PKG between 300 and 450 nm at native and (partly) denatured states in the absence and presence of cGMP, respectively. In the absence of cGMP, no large differences in intensity were observed at different urea concentrations. However, in the presence of cGMP, the intensity increased between 0 and 4 M urea and later decreased again between 4 and 8 M urea. A clear shift in maximal emission wavelength (MEW) between the native and the fully denatured state (0 and 8 M urea) was detected. In the absence of cGMP, a shift of 13.5 nm was observed between 332.8 ± 1.1 nm (0 M urea) and 346.3 ± 1.7 nm (8 M urea); compare maxima of spectrum A and E in Fig. 1A. In the presence of cGMP, a similar red shift of 12.7 nm between 333.6 ± 0.6 nm (0 M urea) and 346.3 ± 1.7 nm (8 M urea) was found (spectrum F and J in Fig. 1B). These MEW shifts are

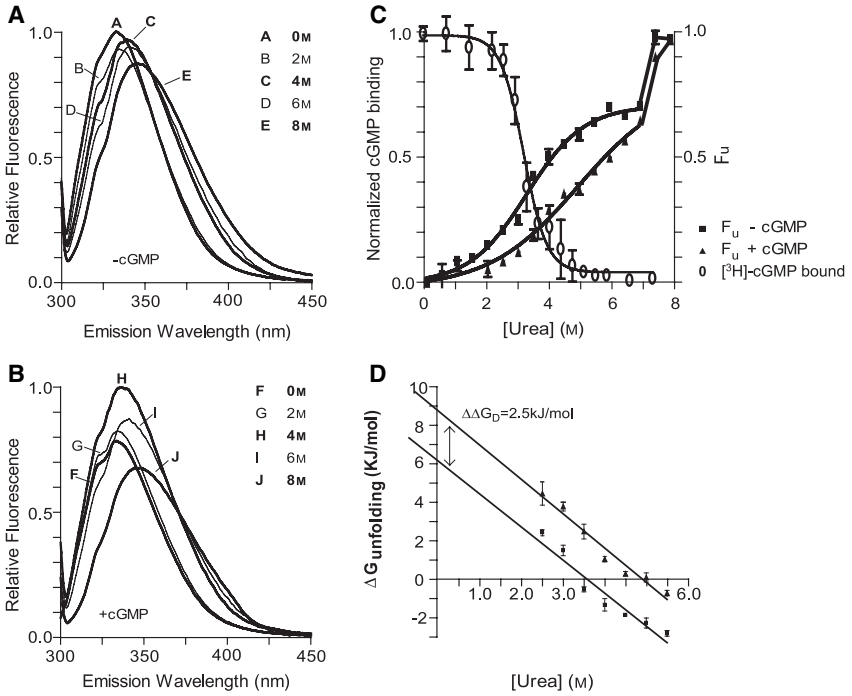

Fig. 1. Influence of cGMP on the stability of PKG during urea unfolding. Fluorescence emission spectra of PKG Iα in the absence (A) and presence (B) of cGMP at native (0 M) and fully denatured (8 M) states, and partially denatured states at 2-M intervals. Lines represent average spectra ($n = 8$ for spectrum A, E, F and J, $n = 3$ for spectrum B, C, D, G, H and I). (C) Unfolding curves of PKG (■) and of PKG + cGMP (▲) based on F_u (relative unfolding state), right axis. Normalized [^{3}H]cGMP binding at different urea concentrations (○), left axis. The maximal cGMP-binding stoichiometry was 1.9 cGMP molecules per monomer PKG. (D) $\Delta\Delta G_D$-values of PKG plotted as a function of urea concentration in the absence (■) and presence(▲) of cGMP.

suitable to measure the unfolding state of PKG [25]. Therefore, we monitored the unfolding behavior of PKG in the presence and absence of cGMP at increasing urea concentrations. This was achieved by calculating the contribution of the unfolding state F_u from the intensity ratio at 332.8 (Apo), 333.6 (cGMP bound) and 346.3 nm (fully denatured), as described in the Experimental procedures. The results are depicted in Fig. 1C; it is clear that, unlike PKA [26], PKG does not unfold through a two-state mechanism. A stable intermediate was observed around a urea concentration of 6.5–7.0 M. Between the concentrations 7 and 8 M there is a second steep increase in F_u that represents the unfolding of the intermediate. By comparing the F_u-values of PKG in the absence and presence of cGMP, it is observed that cGMP affects only the unfolding of PKG between 0 and 6.5 M urea, where the cGMP-bound PKG shows a consistently lower F_u, indicating that cGMP stabilizes PKG. Apparently, at higher concentrations (7–8 M), where the F_u-values are the same, cGMP no longer exerts a stabilizing effect. As protein unfolding intermediates at elevated urea concentrations usually represent molten globule states, their apparent stability bears no relevance for the cGMP-dependent effects we were interested in, in the context of this experiment.

To show that cGMP-binding affects only PKG's stability at urea concentrations between 0 and 6.5 M, we employed [^{3}H]cGMP binding studies. PKG was incubated with radiolabeled cGMP at different concentrations of urea. A binding stoichiometry of 1.9 [^{3}H]cGMP molecules per PKG monomer was observed. The normalized [^{3}H]cGMP-binding curve is represented in Fig. 1C (normalization to the maximal binding concentration). Fitting a sigmoidal curve to the data points indicated that the EC_{50} of the binding curve is present at 3.2 ± 0.3M urea. Binding of cGMP to either binding site was lost above 5.5 M urea. Intriguingly, there seems to be an offset between the midpoint of unfolding in the presence of cGMP (4.5 M urea) and the EC_{50} of the [^{3}H]cGMP binding curve. It would be expected that the EC_{50} of the binding curve would coincide with the midpoint of denaturation of $PKG_2(cGMP)_4$. This is likely to be caused by the different conditions under which both experiments were performed (0 °C versus room temperature and different buffers). Nevertheless, this curve shows that cGMP binding is lost during urea unfolding, as was already expected from the different unfolding behavior of cGMP-saturated and cGMP-free PKG at these urea concentrations. This finding shows that cGMP can only exert an effect on PKG's stability below 6.5 M urea and does not have any influence on the stability of the intermediate that unfolds between 7 and 8 M urea.

To numerically compare the effect of cGMP binding on the stability of the kinase, we fitted a sigmoidal curve onto the unfolding data between 0 and 7 M urea,

from which the midpoints of unfolding (C_m) were calculated to be 3.3 ± 0.1 M (PKG) and 4.5 ± 0.3 M (PKG + cGMP), respectively. Thus, these results indicate that cGMP stabilizes the protein.

To quantify the established stabilization induced by cGMP, in Fig. 1D, the ΔG_D values (free energy of denaturation) in the transition regions (2.5–5.5 M urea) were calculated and plotted as a function of the urea concentration. Extrapolation of this linear dependency yielded the ΔG_{H_2O}-value (free energy of unfolding in water). These were: 6.2 ± 0.5 kJ·mol^{-1} (PKG) and 8.7 ± 0.4 kJ·mol^{-1} (PKG + cGMP). These results show that cGMP stabilizes the unfolding of PKG by a $\Delta\Delta G_D$ of 2.5 kJ·mol^{-1}.

Stoichiometry and catalytic activity of wild-type PKG, Δ1-77 and R77L

As bovine PKG Iα harbors eight tryptophans that are not evenly spread throughout the protein (Trp positions are 189, 288, 446, 515, 541, 617, 623 and 666), the tryptophan quenching technique can only provide a general concept of the cGMP-induced stability. However, this technique is quite powerful to elucidate conformational changes in response to ligand binding [26,27]. To elucidate which domains of PKG are stabilized, we utilized a limited proteolysis technique combined with MS on wild-type PKG and two mutants, PKG Δ1-77 and PKG R77L. All PKG forms were over-expressed and purified from Sf9 insect cells using methods described previously [28–30]. As a means of quality assurance, we analyzed the proteins by liquid chromatography-coupled (LC-MS) and native MS. The measured masses obtained by LC-MS are depicted in Table 1. Using the denaturing conditions (0.06% trifluoroacetc acid and acetonitrile) of a typical LC-MS approach, we observed only PKG monomers. Their molecular masses could be measured with an accuracy of a few Daltons, as depicted in Table 1. For all three proteins, the expected theoretical masses matched to the measured masses, assuming, as described previously [31], that the N-terminal methionine was removed, threonine 516 was fully phosphorylated and the N-terminus acetylated. We also measured the two PKG mutants by native MS (Fig. 2) [32]. Prior to measurement, the proteins were buffer exchanged into aqueous ammonium acetate solutions in the absence and presence of cGMP. Such an approach allows the analysis of noncovalent protein complexes, and thus the analysis of the stoichiometry of protein complexes [31,33,34]. Figure 2A,B shows the spectra obtained for the Δ1-77 mutant in the absence and presence of cGMP. From the mass, depicted in Table 1, it is obvious that Δ1-77 is a monomeric protein. The R77L spectra are in very close agreement with the spectra obtained for wild-type PKG by Pinkse *et al.* [31] and demonstrate that R77L is indeed a dimeric protein (Fig. 2C) that can bind four cGMP molecules (Fig. 2D). As described for wild-type PKG earlier [31], the native ESI-MS spectrum of R77L showed that the initial cyclic nucleotide occupancy was minimal, only a very small shoulder, representing the presence of no more than 5% of R77L dimer with one cyclic nucleotide bound (either cGMP or cAMP, the first originating from the Sf9 cells, the latter from the cAMP used during the purification of the protein). The cyclic nucleotide content of the recombinantly expressed Δ1-77 was higher; from the native ESI-MS spectra an estimated 70% of Δ1-77 contained one cyclic nucleotide. Even extensive dialysis could not further remove the remaining bound cyclic nucleotide from the monomeric form. Saturation with cGMP increased the stoichiometry for both mutants to full cGMP occupation, i.e. two for the Δ1-77 monomer and four for R77L

Table 1. Properties of wild-type PKG Iα, Δ1-77 (± cGMP) and R77L. ND, not determined.

Kinetic constants	Wild-type	R77L	Δ1-77	Δ1-77 + cGMP
K_a (cGMP) (μM)[a]	0.063 ± 0.002	0.186 ± 0.033	ND	ND
K_m (with W15-peptide) (μM)[a]	1.53 ± 0.29	1.49 ± 0.08	1.87 ± 0.08	1.62 ± 0.18
V_{max} (μmol·mg·min^{-1})[a]	6.1 ± 2.1	8.0 ± 2.2	8.0 ± 1.5	7.9 ± 0.4
Fold stimulation	9.9 ± 0.1	9.4 ± 0.3	1.0 ± 0.02	
Native PAGE results				
Stoichiometry	Dimer	Dimer	Monomer	Monomer
MS results				
Stoichiometry (native ESI-MS)	Dimer[b]	Dimer	Monomer	Monomer
Average mass calculated (Da)[b]	152819.2	152733.1	67341.2	–
Mass measured LC-ESI-MS	76408.4 ± 3.0	76368.2 ± 1.6	67341.5 ± 1.1	–
Mass measured ESI-MS (native) (Da)	152883[c]	152886	67895	–

[a] W15-peptide TQAKRKKSLAMA [30]. [b] Based on acetylation of N-terminus, phosphorylation of Thr516 and removal of N-terminal methionine. [c] As previously measured [31].

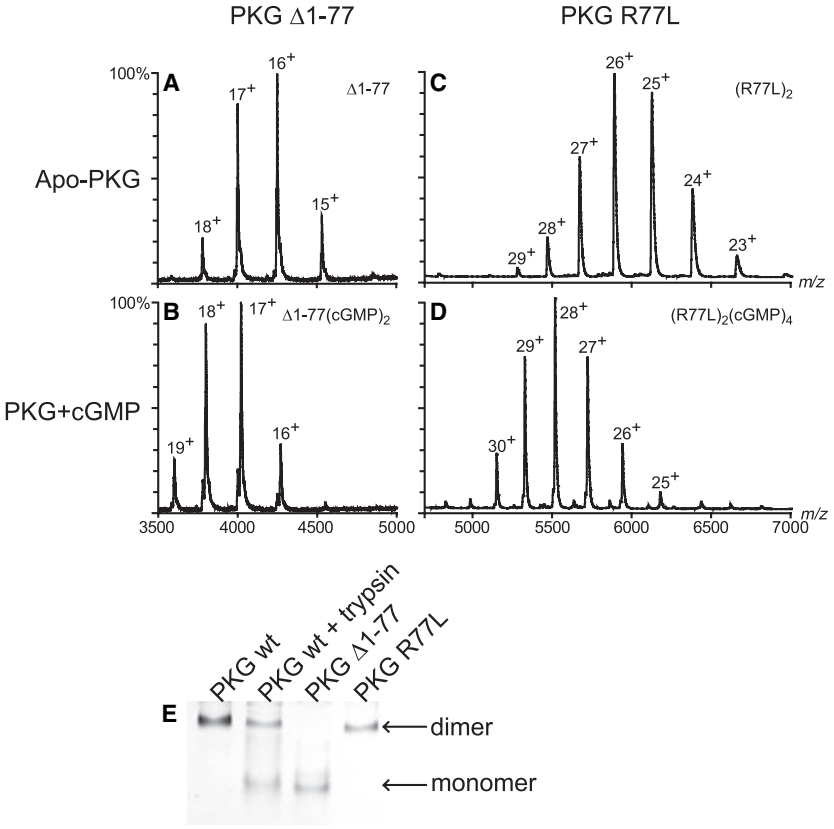

Fig. 2. Native ESI-MS with PKG. Native ESI-MS spectra of PKG Δ1-77 in the absence (A) and presence (B) of 20 μM cGMP and PKG R77L in the absence (C) and presence (D) of cGMP. The *m/z* envelopes are shown. The corresponding deconvoluted masses for each of these species are listed in Table 1. (E) Coomassie blue-stained native PAGE of the different PKG mutants.

dimer (Fig. 2). Interestingly, for both forms of PKG, there is a shift of the envelope to a lower *m/z* upon cGMP binding, i.e. more charges are present on the proteins. This may be indicative of a conformational change that shows a higher charge, meaning a higher exposure of positively charged amino acids. Native gel electrophoresis experiments confirmed that wild-type and R77L PKG are dimeric and Δ1-77 PKG is a monomeric species (Fig. 2E).

The mass spectrometric results described above confirm the proper expression of the three PKG variants, and resolve their oligomeric status. To further validate the recombinant expressed wild-type and mutant PKG proteins, we evaluated their catalytic activities using the model substrate W15 (TQAKRKKSLAMA) [30]). These results are also summarized in Table 1. Within experimental error, the K_m, V_{max} and fold stimulation (the ratio of full over basal activity) for the wild-type PKG and the site-directed mutant R77L were identical. Also, no major changes in K_m and V_{max} were observed for the deletion mutant Δ1-77. The fold stimulation for Δ1-77 was 1.0, as expected, as this N-terminal deletion mutant is known to be constitutively active and independent of cGMP binding. Additionally, we investigated the activation constant ($K_{a,cGMP}$) of PKG. The $K_{a,cGMP}$ of the R77L mutant shifted about threefold up, from 63 to 186 nM, when compared with wild-type PKG. For Δ1-77 no $K_{a,cGMP}$ was determined as it is constitutively active. All these data together confirm that the expressed PKG variants were properly expressed and biologically active. For wild-type PKG the values obtained for catalytic activity and cGMP binding as well as oligomeric state are in agreement with results previously published [4,30].

Limited proteolysis of wild-type PKG in the absence and presence of cGMP

To probe the influence of cGMP binding on the domain stability of the three PKG variants, limited proteolysis was applied, using trypsin, in combination with 1D SDS/PAGE and LC-ESI-MS. Figure 3A,B shows the limited proteolysis results for wild-type PKG in the absence and presence of cGMP, respectively, as monitored by 1D gel electrophoresis. As expected, in Fig. 3A, wild-type PKG was initially only found as a single band at 76 kDa ($t = 0$ min). In the absence of cGMP, limited proteolysis yielded two major degradation products over time (1–30 min) at ~67 and 55 kDa. The 67-kDa fragment was identified as the Δ1-77

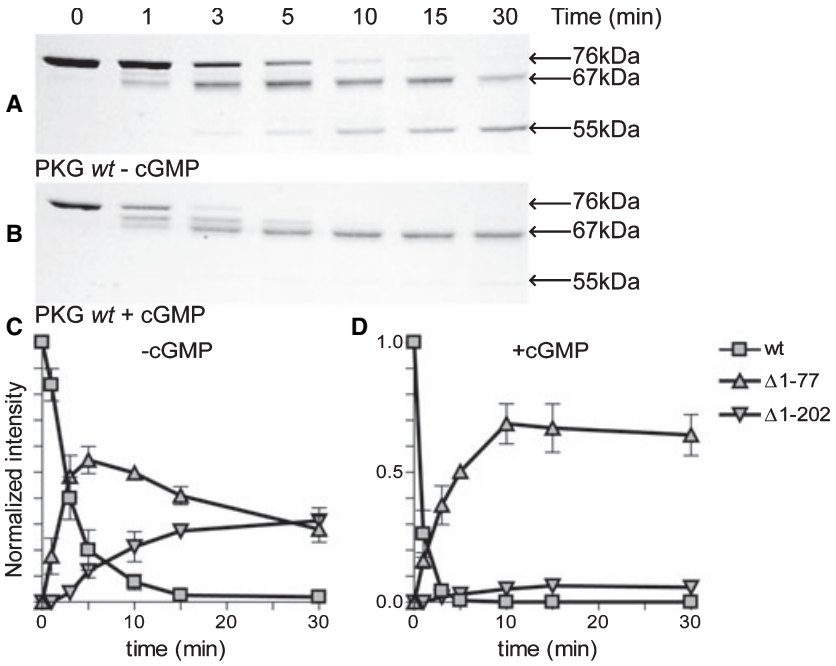

Fig. 3. Influence of cGMP on the partial proteolysis pattern of PKG. A typical example of the time-resolved limited proteolysis of wild-type PKG Iα in the absence (A) and presence (B) of cGMP at different time points of trypsin digestion at 37 °C is shown. In-gel quantification of different digestion products during trypsin digestion of wild-type PKG Iα in the absence (C) and presence (D) of cGMP ($n = 3$). □, full-length PKG; △, PKG Δ1–77 fragment; and ▽, PKG Δ1–202 fragment.

product and the 55-kDa fragment as Δ1-202 by LC-MS (Fig. 4), in agreement with earlier studies [4,16,17]. In the presence of cGMP, the degradation pattern altered significantly (Fig. 3B). Two major degradation products over time were observed at ~70 and 67 kDa. Also, cGMP significantly increased the proteolysis rate. This is further illustrated in Fig. 3C,D, where the semiquantified intensities of the bands at 76 (wild-type), 67 (Δ1-77) and 55 kDa were plotted against time. Extrapolation of these graphs revealed that the half-life of wild-type PKG is decreased more than three-fold upon addition of cGMP, from 2.5 to 0.8 min. In addition, the presence of cGMP significantly reduces the formation of the 55-kDa fragment, thus relatively stabilizing the 67-kDa fragment.

Using LC-ESI-MS, we set out to identify the cleavage products of wild-type PKG formed during limited proteolysis in more detail. Representative examples of such LC-ESI-MS experiments are depicted in Fig. 4. In the initial run (run 1, bottom), we analyzed untreated wild-type PKG. We observed just a single peak in the chromatogram (at $R_t = 31$ min), for which we obtained *m/z* signals corresponding to intact wild-type PKG (see also Table 1 for the molecular mass). When we initiated proteolysis for 5 min, the chromatogram showed specific differences (run 2). Several smaller fragments eluted simultaneously at an approximate retention time of $R_t = 24$ min. These could be identified by their mass as four different small N-terminal cleavage products: 1–56 (6711.7 ± 0.3 Da), 1–59 (7070.7 ± 0.7 Da), 1–71 (8372.7 ± 0.4 Da) and 1–77 (9128.3 ± 0.7 Da), as depicted in the inset of Fig. 4. These N-terminal fragments all confirmed the above-stated N-terminal acetylation and elimination of the first methionine amino acid. At the retention time of the intact wild-type PKG ($R_t = 31$ min), we detected, together with the full-length PKG of 76 kDa (A-ions), another co-eluting fragment of 67299.3 ± 1.1 Da (B-ions) (Fig. 4, run 2, middle). The mass of this fragment corresponds well with the calculated mass of PKG cleaved at R77 (67299.2 Da), thereby confirming that the 67 kDa fragment observed in Fig. 2 is PKG Δ1-77. Following prolonged incubation with trypsin (30 min, run 3, top), we observed the same N-terminal fragments and the co-elution of primarily Δ1-77 and a fragment of 53076.7 ± 1.7 Da (C-ions). The mass of this fragment points to a cleavage of PKG at R202 ($M_{calc} = 53075.4$ Da). In agreement with the data depicted in Fig. 3A, no full-length PKG was detectable at this time point. When the limited proteolysis step was performed in the presence of cGMP, a larger variety of fragments co-eluted at an approximate R_t of 31 min, whereby we could clearly identify Δ1-77, Δ1-59 (69315.53 ± 1.26 Da) and Δ1-71 (68011.93 ± 3.27) as major products (data not shown). Under these conditions, in contrast to the experiments without cGMP, no Δ1-202 was detected at any time point. Therefore, all these LC-ESI-MS data are in perfect agreement with the 1D gel data depicted in Fig. 3; however, the latter give immediate and much more detailed information about the actual site of cleavage and the identity of the formed fragments.

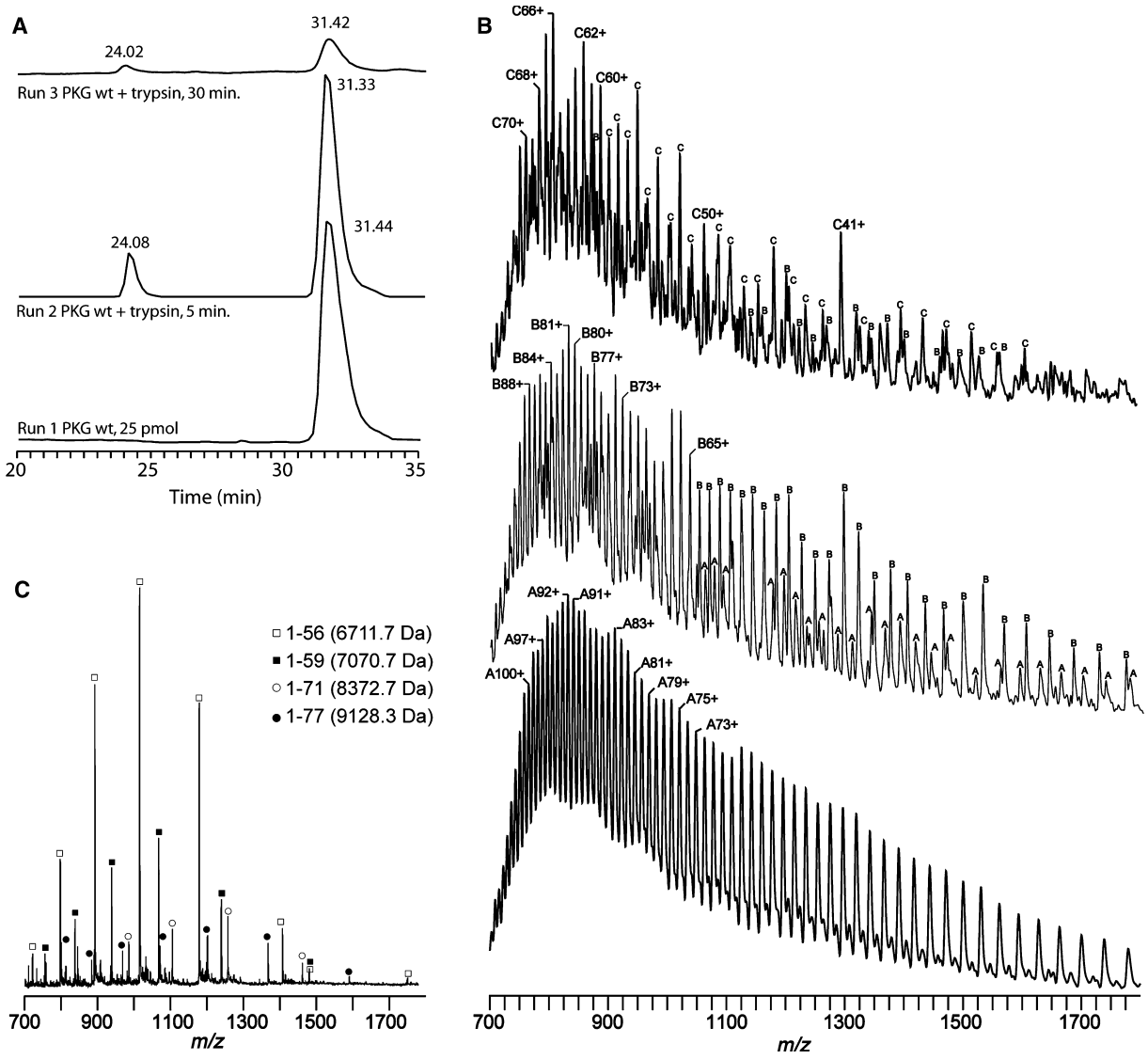

Fig. 4. LC-ESI-MS of trypsin digested wild-type PKG. Total ion count (TIC) chromatograms (A) of untreated PKG (run 1), PKG treated with trypsin for 5 (run 2) and 20 min (run 3), respectively. (B) *m/z* signals for the TIC-peaks at $R_t = 31.4$ min in runs 1, 2 and 3 (ions: A, wild-type PKG; B, PKG Δ1-77; and C, PKG Δ1-202). (C) Mass spectrum of small N-terminal fragments eluting at $R_t = 24.0$ min in runs 2 and run 3.

Limited proteolysis of PKG-mutants

Limited proteolysis experiments with the Δ1-77 PKG deletion mutant fitted well to wild-type PKG. Cleavage at R202 occurred in absence of, but not in the presence of cGMP, as illustrated in Fig. 5A,B. Overall, it was observed that the Δ1-77 degradation was much slower, indicating that the formation of PKG Δ1-201 from PKG Δ1-77 is slower than the cleavage at R77. Formation of PKG Δ1-202 in absence of cGMP was confirmed by LC-ESI-MS (data not shown).

Similar experiments with the site-directed R77L mutant revealed that, although this mutant is catalytically very similar to wild-type PKG, it is much more stable (Fig. 5C,D). In the absence of cGMP, most of the R77L is intact after 30 min, as shown on the gel. In the LC-ESI-MS run, only some minor Δ1-202 could be detected and thus seems to be the only specific cleavage product. LC-ESI-MS experiments even after prolonged incubation times (1 h), revealed no major other cleavage products (data not shown). Addition of cGMP had a remarkable effect on the stability of the R77L mutant. Now, a rather rapid degradation was observed (Fig. 5D), whereby LC-ESI-MS data verified the formation of three large fragments; Δ1-56 (69674.28 ± 0.84 Da), Δ1-59 and Δ1-71, but

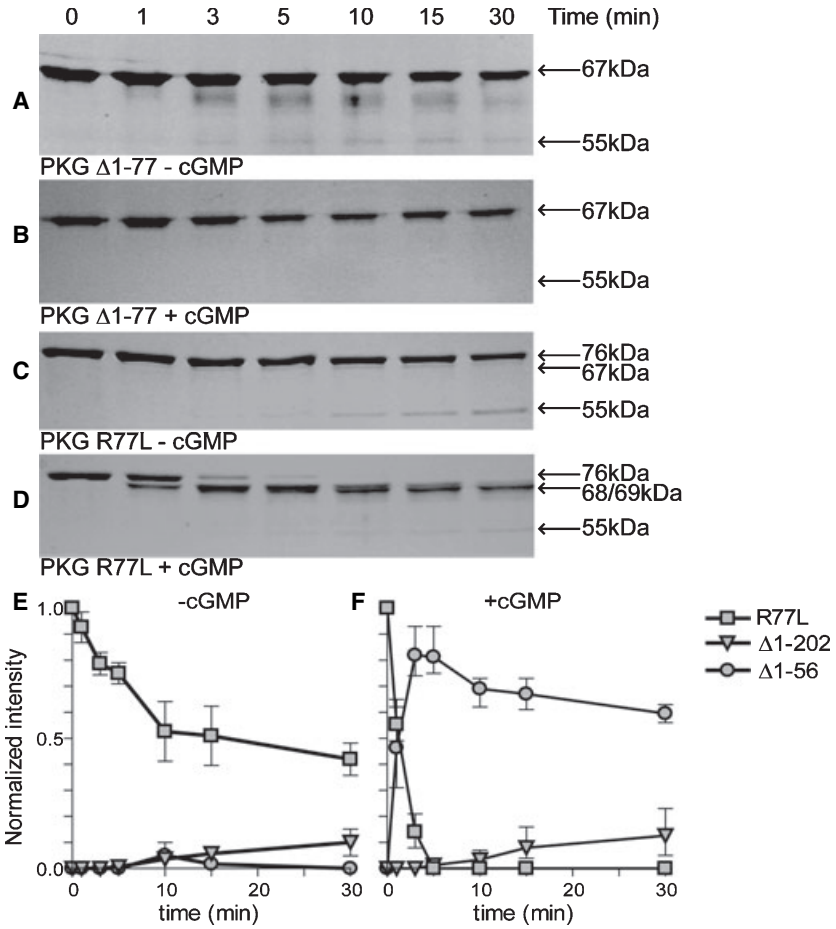

Fig. 5. Partial proteolysis patterns of PKG mutants Δ1-77 and R77L. Typical example of a limited proteolysis experiment with PKG Iα Δ1-77 in the absence (A) and presence (B) of cGMP at different time points. The same experiment with PKG R77L in the absence (C) and presence (D) of cGMP. Quantification of different digestion products over time for the R77L mutant in the absence (E) and presence (F) of cGMP ($n = 3$). □, full-length PKG R77L; ▽, PKG Δ1–202; ○, PKG Δ1–56.

not Δ1-202, in agreement with wild-type. The stability of the R77L mutant is further illustrated by the relative quantification graphs depicted in Fig. 5E,F. Extrapolation revealed that the half-life of R77L is approximately 17 min. This is reduced to about 1 min upon cGMP stimulation.

Discussion

Urea unfolding studies utilizing the regulatory-subunit of PKA (PKA-R) showed that cAMP had a stabilizing effect on the protein [26,27]. Moreover, all PKA-R crystal structures were resolved with bound cyclic nucleotide [35,36]. This suggests that in analogy to PKA, cGMP binding to PKG also has a stabilizing effect on the overall structure. The PKA holoenzyme structure is, so far, the only one without bound cyclic nucleotides on the R-subunit [23]. Therefore, it was suspected that cGMP would play an important role in PKG's overall stability, just as cAMP does for PKA. Even though, PKG does not unfold through a two-state mechanism, like PKA, our results show a global stabilizing effect of cGMP on the structure of the protein (Fig. 1C,D). Recently, Wall *et al.* [20] observed that cGMP induces a significant conformational change to a monomeric form of PKG Iβ that elongates the protein by ~30%. We expected to be able to monitor this conformational change in the PKG Iα dimer by fluorescence spectroscopy. However, under native conditions (0 M urea), we observed no significant effect of cGMP on the MEW (332.8 ± 1.1 nm versus 333.6 ± 0.6, compare MEW in Fig. 1A, curve A and Fig. 1B, curve F). Apparently, the conformational change induced by cGMP does not influence the fluorescence to the extent for it to be detected under the conditions employed in this study. Either none of the tryptophans is sufficiently affected, or two or more tryptophan fluorescence alterations cancel each other out. Although cGMP binding greatly influences the conformation of the N-terminus, this domain does not contain any tryptophans. This could also be an explanation for the absence of a significant MEW shift upon binding of cGMP to native PKG. Whether cGMP would have a stabilizing effect on the structure of PKG was subsequently determined. If we assume that PKG is completely denatured at 8 M urea, then

the F_u curve shows that unfolding of PKG goes through a stable, molten globule intermediate, which is present around 6.5–7.0 M urea. It no longer binds cGMP and its further unfolding is not affected by it. It is also possible that the intermediate state, present at F_u of 0.70, contains a strong hydrophobic domain that is only unfolded at elevated urea concentrations.

It was established earlier that cGMP renders the N-terminus of PKG more susceptible towards proteolytic cleavage, especially in the hinge region [12,22]. Our results using wild-type PKG not only confirm this finding, but suggest that, based on our limited proteolysis data, only a limited region around position R77 (the hinge region) is exposed to the surface in the presence and absence of cGMP, as the proteolytic efficiency of trypsin only dropped 2.5-fold in the absence of cGMP. The labile nature of the R77 site in the hinge region prompted us to mutate this arginine into a leucine, thereby inactivating trypsin activity at this particular position. This resulted in a complete stabilization of the enzyme towards trypsin in the absence of cGMP. In addition, Chu *et al.* [22] found F80 to be the major target of chymotrypsin in the hinge region of wild-type PKG Iα in the presence and absence of cGMP.

Taken together, our findings suggest that the exposed part of the hinge region around R77 in the nonactivated state is rather small, as, for instance, nearby R71, K85, R88 and K90 are not cleaved when PKG is in the inactivated conformation, as confirmed by our LC-ESI-MS experiments. Even more surprising is the apparent stability of R81 and K82, as they are in direct vicinity of the reported chymotrypsin labile F80 residue [22]. Evidently, the exposed part of the N-terminus in the nonactivated state is likely to be limited to a small region between R71 and F80, suggesting that the remainder of the protein is in a very tight conformation.

Another interesting observation concerning the cGMP-free R77L-PKG is that the mutation not only exerts an effect on the stability of the hinge region, but also on the first cGMP binding pocket, as the formation of Δ1-202 PKG from R77L PKG is almost negligible in the absence of cGMP when compared with wild-type PKG (compare graphs in Fig. 3C and Fig. 5E). This gives rise to the hypothesis that the N-terminus in the nonactivated state is in close proximity to the first cGMP binding pocket, which is where R202 resides. Interestingly, Chu *et al.* [22] found residue M200 of wild-type PKG Iα to be the major proteolytic site in the first cGMP binding pocket. The fact that autophosphorylation at typical residues like S72 and T58 of PKG [37,38] has a profound effect on the kinetics of cGMP-binding to the first cGMP binding pocket [4] is in close agreement with our finding, as these phosphorylation events are likely to change the conformation of the N-terminus.

In the presence of cGMP, the stabilizing effect of the R77L mutation is completely abolished and the protein behaves exactly like wild-type PKG. Now, with the R77 not available, the more exposed N-terminus is cleaved at alternative positions closer to, or in, the auto-inhibitory domain, such as R71, R59 and R56. The R202 position is now protected by cGMP binding, just as in wild-type PKG [22]. The LC-MS data obtained for wild-type and R77L PKG now identified the extent of additional N-terminus exposure upon cGMP binding. Besides the increased rate of Δ1-77 formation, it is now also apparent that the cGMP-induced exposure of the N-terminus reaches much further towards the N-terminus, and also affects the auto-inhibitory region around I63.

In summary, our results lead us to a model as proposed in Fig. 6, where a small part of the hinge region is exposed in the absence of cGMP (with R77 and F80 [22]). In addition to the interaction of the auto-inhibitory domain with the catalytic domain through I63 [39], the position of the N-terminus in close proximity to the cGMP-binding domains is depicted. Upon

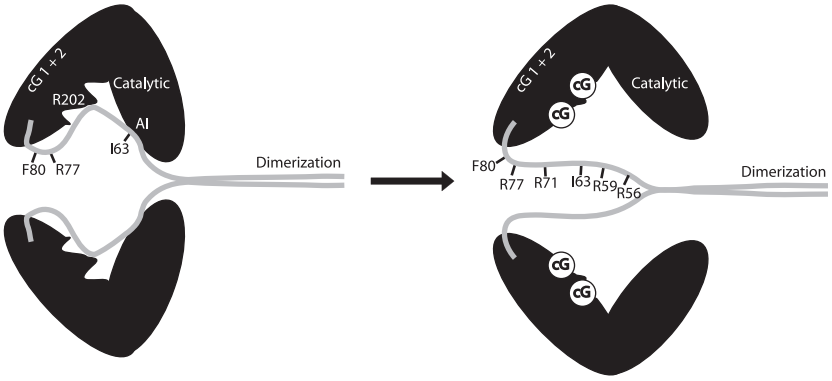

Fig. 6. Model of the proposed stability switch in PKG Iα. Model of PKG with an emphasis of the N-terminal hinge region (amino acids 71–80) in the nonactive and active states. Trypsin-susceptible arginines are depicted, as well as the previously described chymotryptic cleavage site F80 [22] and the important I63 for auto-inhibition [39]. The conformational change induced through binding of cGMP (cG) increases the surface accessibility of the hinge region.

binding of cGMP, both interactions are relaxed as proven by the susceptibility of the arginines within the auto-inhibitory domain (R59 and R56). Our results suggest that the hinge region, which we suggest to reside between R71 and F80, acts as a stability switch for the entire protein as mutation of the only trypsin sensitive site in it (R77) completely stabilizes PKG in the absence of cGMP.

Experimental procedures

Oligonucleotides were obtained from Sigma Genosys (The Woodlands, TX, USA). Restriction enzymes, Baculovirus expression system, Sf9 cells and insect cell medium were from Invitrogen (Carlsbad, CA, USA). HPLC-S gradient grade acetonitrile was purchased from Biosolve (Valkenswaard, the Netherlands) and high purity water obtained from a Milli-Q system (Millipore, Bedford, MA, USA) was used for all experiments. Cyclic-3′,5′-guanosine monophosphate (cGMP) was purchased from Biolog (Bremen, Germany), ^{3}[H]-cGMP was purchased from ICN Biomedicals (Irvine, CA, USA) and had a specific activity of 30 Ci·mmol^{-1}. All other chemicals were purchased from commercial sources in the highest purity unless stated otherwise. The W15 peptide, TQAKRKKSLAMA, was a gift from W. Tegge [40].

Protein preparation

Bovine PKG was recombinantly expressed in Sf9-insect cells according to Feil *et al.* [28] and then purified according to the method described by Dostmann *et al.* [30]. The Δ1-77 and R77L mutants were generated with bovine wild-type PKG Iα cDNA as a template [41]. The obtained constructs were ligated into pFastBacI vector (Invitrogen, Carlsbad, CA, USA). Prior to transformation, all constructs were verified by DNA sequencing on an ABI 310 Prism Genetic Analyzer at the DNA-Analysis Core Facility, University of Vermont (Burlington, VT, USA). Preparation of bacumid DNA, transfection of Sf9 cells and two rounds of Baculovirus amplification were performed according to the manufacturer's protocol. Expression of both mutants in Sf9 cells was confirmed by western blotting with an antibody that recognizes the C-terminal part of PKG [42].

Tryptophan fluorescence measurements

The tryptophan fluorescence methods were adapted from Leon *et al.* [26], as follows. PKG was diluted to a final concentration of 250 nM in buffer A (5 mM Mops, pH 6.8; 0.5 mM EDTA, 100 mM KCl, 5 mM 2-mercaptoethanol) with different concentrations of urea (0–8 M) and left at room temperature for 2 h prior to measurements. To find the MEW at an excitation wavelength of 293 nm, samples were measured in the native (0 M urea) and completely unfolded state (8 M urea) subsequently, both in the presence and absence of cGMP (60 μM). MEWs for PKG at 8 M/0 M, respectively, were observed at 346.2/332.8 nm (PKG) and 346.4/333.6 nm (PKG + cGMP). Background noise was subtracted from the spectra by measuring the same samples prior to addition of PKG. The intensity ratio at the specific MEW wavelengths, $R(I_{MEW,8\ M}/I_{MEW,0\ M})$, was used to follow the relative shift in wavelength at different urea concentrations (0–8 M in 0.5-M intervals). Generation of the fractional denaturation curve at different urea concentrations can now be achieved by using these intensity ratios in Eqn 1:

$$F_U = 1 - \left(\frac{R_0 - R_D}{R_N - R_D}\right) \quad (1)$$

where F_U is the fraction of unfolding, R_0 is the observed intensity ratio at various urea concentrations, R_N is the fluorescence intensity ratio at native conditions (0 M), and R_D is the ratio at denatured conditions (8 M) [25].

The ΔG_D-values were calculated for a two-state model by utilizing the assumption that $F_N + F_U = 1$, where F_N is the fraction of native protein [43], then:

$$\frac{F_U}{F_N} = K_D$$

and

$$K_D = e^{\frac{-\Delta G_D}{RT}}$$

then

$$-RT\ln\left(\frac{F_u}{F_N}\right) = \Delta G_D \quad (2)$$

By using an extrapolation method [43], the $\Delta G_D^{H_2O}$ -values (conformational stability in absence of denaturant) was then calculated.

[^{3}H]-cGMP binding assay

To assay the capability of PKG wild-type to bind cGMP at different urea concentrations, the protein (50 nM) was dissolved in buffer B [50 mM Mes, 0.4 mM EGTA, 1 mM $MgCl_2$, 10 mM NaCl, 0.5 mg·mL^{-1} bovine serum albumin, 10 mM dithiothreitol, 0.2 μM [^{3}H]-cGMP (ICN Biomedicals)] with different concentrations of urea (0–7.3 M) and incubated on ice for 2 h. The protein was then precipitated in 3 mL of ice-cold saturated $(NH_4)_2SO_4$ solution and incubated for another 5 min on ice. Samples were subsequently vacuum filtrated over an 0.22 μm nitrocellulose membrane. Filters were washed twice with 3 mL ammonium sulfate before addition of 10 mL toluene-based scintillation fluid. Samples were subsequently assayed for radioactivity in a scintillation counter. A negative control was performed using a protein free sample.

Kinetic characterization of mutants

Determination of the activation constant (K_a) for cGMP on recombinant bovine wild-type PKG and R77L was adapted from Landgraf *et al.* [4] and Dostmann *et al.* [30]. Briefly, 16 μM W15 (TQAKRKKSLAMA) was phosphorylated by PKG (1 nM) in the presence of different cGMP concentrations (0.006–3.1 μM) and 1 mM ATP. K_m values with the substrate peptide W15 for all mutants were determined according to Dostmann *et al.* [30]. All assays were performed at least in triplicate and V_{max}-values were determined from both assays.

Native gel electrophoresis

Native gel electrophoresis was performed as described by Chu *et al.* [22]. Briefly, proteins were run on a 9.5% polyacrylamide separating gel in absence of sodium dodecylsulfate at 4 °C. Gels were run at 5 mA for 2 h and subsequently at 10 mA for an additional 5 h. A 5% stacking gel was used and proteins were stained using Coomassie brilliant blue staining.

Native ESI-MS

Sample preparation and electrospray (ESI)-MS measurements under native conditions [33] were performed on a Micromass LC-T time-of-flight (TOF) instrument equipped with a 'Z-Spray' nanoflow ESI source (Micromass UK Ltd, Manchester, UK), as described by Pinkse *et al.* [31]. Briefly, the PKG solutions were analyzed using in-house pulled and gold-coated borosilicate glass needles. Typical ESI-TOF-MS parameters were as follows: capillary voltage 1.0–1.5 kV, sample cone voltage 100–200 V, extraction cone voltage 50–100 V, source pressure 9.0 mbar and TOF analyzer pressure 1.3×10^{-6} mbar. Spectra were recorded in the positive ion mode between m/z 200–10 000. For sample preparation, PKG was buffer exchanged to a volatile buffer containing 200 mM ammonium acetate (pH 6.7) with Ultrafree-0.5 centrifugal filter units (5000 NMWL; Millipore, Bedford, MA, USA). The final PKG concentration was 5 μM. cGMP (20 μM final concentration), when applied, was also dissolved in this buffer and preincubated with PKG on ice for 5 min before analysis by ESI.

Limited proteolysis analyzed by SDS/PAGE

In a total volume of 40 μL, 3 μg PKG (1 μM) was incubated in the presence and absence of 20 μM cGMP in buffer A (30 mM Hepes, 2 mM EDTA, 15 mM 2-mercaptoethanol) for 5 min on ice and subsequently subjected to 15 ng trypsin for 1, 3, 5, 10, 15 and 30 min at 37 °C. The digest was terminated by addition of 10 μL SDS/PAGE sample buffer and heated at 95 °C for 3 min. Samples were then separated by SDS/PAGE on a 10% acrylamide gel and stained with Coomassie brilliant blue. After destaining, the different gel bands were imaged and quantified based on intensity with a Bio-Rad Gelquant densitometer (Bio-Rad, Hercules, CA, USA).

Identification of proteolytic fragments by LC-ESI-MS

Identification of the differently formed proteolytic fragments was achieved by digesting 2 μg PKG with 20 ng trypsin for 5 and 30 min at 37 °C. Subsequent separation by reversed-phase HPLC was performed on a system equipped with two Shimadzu LC-10AD VP pumping units, a Shimadzu SPD10A VP UV-detector set at 280 nm (Shimadzu, 's-Hertogenbosch, the Netherlands) and a C18 column (Vydac, Hesperia, CA, USA). Mobile phases were 0.06% trifluoroacetic acid (mixture A) and 90% acetonitrile with 0.06% trifluoroacetic acid (mixture B), both in milliQ water. A gradient from 10 to 80% of mixture B was set over a period of 35 min at a flow of 600–700 $\mu L \cdot min^{-1}$. A split flow of $\sim$50 $\mu L \cdot min^{-1}$ was directly coupled to the ESI-TOF-MS mentioned above. Operating parameters of the ESI-TOF-MS were as follows: capillary voltage 3 kV, sample cone voltage 25 V, extraction cone voltage 1 V, source block temperature 300 °C, source pressure 2.0 mbar and TOF analyzer pressure 6.2×10^{-7} mbar. Spectra were recorded in the positive ion mode and monitored between m/z 500–4000. Calibration was achieved by direct injection of a horse heart myoglobin solution (5 $mg \cdot mL^{-1}$; Sigma, Zwijndrecht, the Netherlands) in 50% of mixture B into the ESI-TOF-MS after the gradient had finished.

Acknowledgements

Martijn Pinkse, Akira Honda, Sander Engels and Christian Nickl are kindly acknowledged for their technical assistance during the experiments described in this manuscript. Financial support was provided by NIH grant HL68891, by the Totman Trust for Medical Research and the Netherlands Proteomics Centre.

References

1 Lincoln TM, Wu X, Sellak H, Dey N & Choi CS (2006) Regulation of vascular smooth muscle cell phenotype by cyclic GMP and cyclic GMP-dependent protein kinase. *Front Biosci* **11**, 356–367.
2 Feil R, Hofmann F & Kleppisch T (2005) Function of cGMP-dependent protein kinases in the nervous system. *Rev Neurosci* **16**, 23–41.
3 Hofmann F, Feil R, Kleppisch T & Schlossmann J (2006) Function of cGMP-dependent protein kinases as revealed by gene deletion. *Physiol Rev* **86**, 1–23.

4 Landgraf W & Hofmann F (1989) The amino terminus regulates binding to and activation of cGMP-dependent protein kinase. *Eur J Biochem* **181**, 643–650.
5 Hofmann F, Gensheimer H-P & Göbel C (1985) cGMP-dependent protein kinase; Autophosphorylation changes the characteristics of binding site 1. *Eur J Biochem* **147**, 361–365.
6 Landgraf W, Hullin R, Göbel C & Hofmann F (1986) Phosphorylation of cGMP-dependent protein kinase increases the affinity for cyclic AMP. *Eur J Biochem* **154**, 113–117.
7 Chu DM, Francis SH, Thomas JW, Maksymovitch EA, Fosler M & Corbin JD (1998) Activation by autophosphorylation or cGMP binding produces a similar apparent conformational change in cGMP-dependent protein kinase. *J Biol Chem* **273**, 14649–14656.
8 Hofmann F, Ammendola A & Schlossmann J (2000) Rising behind NO: cGMP-dependent protein kinase. *J Cell Sci* **113**, 1671–1676.
9 Vo NK, Gettemy JM & Coghlan VM (1998) Identification of cGMP-dependent protein kinase anchoring proteins (GKAPs). *Biochem Biophys Res Commun* **246**, 831–835.
10 Yuasa K, Michibata H, Omori K & Yanaka N (1999) A novel interaction of cGMP-dependent protein kinase I with troponin T. *J Biol Chem* **274**, 37429–37434.
11 Busch JL, Bessay EP, Francis SH & Corbin JD (2002) A conserved serine juxtaposed to the pseudosubstrate site of type I cGMP-dependent protein kinase contributes strongly to autoinhibition and lower cGMP affinity. *J Biol Chem* **277**, 34048–34054.
12 Francis SH, Smith JA, Colbran JL, Grimes K, Walsh KA, Kumar S & Corbin JD (1996) Arginine 75 in the pseudosubstrate sequence of type Ibeta cGMP-dependent protein kinase is critical for autoinhibition, although autophosphorylated serine 63 is outside this sequence. *J Biol Chem* **271**, 20748–20755.
13 Ruth P, Pfeifer A, Kamm S, Klatt P, Dostmann WRG & Hofmann F (1997) Identification of the amino acid sequences responsible for high affinity activation of cGMP kinase Ia. *J Biol Chem* **272**, 10522–10528.
14 Reed RB, Sandberg M, Jahnsen T, Lohmann SM, Francis SH & Corbin JD (1996) Fast and slow cyclic nucleotide-dissociation sites in cAMP-dependent protein kinase are transposed in type Ibeta cGMP-dependent protein kinase. *J Biol Chem* **271**, 17570–17575.
15 Corbin JD & Doskeland SO (1983) Studies of two different intrachain cGMP-binding sites of cGMP-dependent protein kinase. *J Biol Chem* **258**, 11391–11397.
16 Monken CE & Gill GN (1980) Structural analysis of cGMP-dependent kinase using limited proteolysis. *J Biol Chem* **255**, 7067–7070.
17 Heil WG, Landgraf W & Hofmann F (1987) A catalytically active fragment of cGMP-dependent protein kinase; occupation of its cGMP-binding sites does not effect its phosphotransferase activity. *Eur J Biochem* **168**, 117–121.
18 Dostmann WRG, Koep N & Endres R (1996) The catalytic domain of the cGMP-dependent protein kinase Ia modulates the cGMP-characteristics of its regulatory domain. *FEBS Lett* **398**, 206–210.
19 Takio K, Wade RD, Smith SB, Krebs EG, Walsh KA & Titani K (1984) Guanosine cyclic-3′,5′-phosphate dependent protein kinase, a chimeric protein homologous with two separate protein families. *Biochemistry* **23**, 4207–4218.
20 Wall ME Francis SH, Corbin JD, Grimes K, Richie-Jannetta R, Kotera J, Macdonald BA, Gibson RR, Trewhella J (2003) Mechanisms associated with cGMP binding and activation of cGMP-dependent protein kinase. *Proc Natl Acad Sci USA* **100**, 2380–2385.
21 Zhao J, Trewhella J, Corbin J, Francis S, Mitchell R, Brushia R & Walsh D (1997) Progressive cyclic nucleotide-induced conformational changes in the cGMP-dependent protein kinase studied by small angle X-ray scattering in solution. *J Biol Chem* **272**, 31929–31936.
22 Chu DM, Corbin JD, Grimes KA & Francis SH (1997) Activation by cyclic GMP binding causes an apparent conformational change in cGMP-dependent protein kinase. *J Biol Chem* **272**, 31922–31928.
23 Kim C, Xuong NH & Taylor SS (2005) Crystal structure of a complex between the catalytic and regulatory (RIalpha) subunits of PKA. *Science* **307**, 690–696.
24 Atkinson RA, Saudek V, Huggins JP & Pelton JT (1991) 1H NMR and circular dichroism studies of the N-terminal domain of cyclic GMP dependent protein kinase: a leucine/isoleucine zipper. *Biochemistry* **30**, 9387–9395.
25 Tandon S & Horowitz PM (1990) The detection of kinetic intermediate(s) during refolding of rhodanese. *J Biol Chem* **265**, 5967–5970.
26 Leon DA, Dostmann WR & Taylor SS (1991) Unfolding of the regulatory subunit of cAMP-dependent protein kinase I. *Biochemistry* **30**, 3035–3040.
27 Leon DA, Canaves JM & Taylor SS (2000) Probing the multidomain structure of the type I regulatory subunit of cAMP-dependent protein kinase using mutational analysis: role and environment of endogenous tryptophans. *Biochemistry* **39**, 5662–5671.
28 Feil R, Müller S & Hofmann F (1993) High-level expression of functional cGMP-dependent protein kinase using the baculovirus system. *FEBS Lett* **336**, 163–167.
29 Pöhler D, Butt E, Meißner J, Müller S, Lohse M, Walter U, Lohmann SM & Jarchau T (1995) Expression, purification and characterization of the cGMP-dependent protein kinase Iβ and II using the baculovirus system. *FEBS Lett* **374**, 419–425.
30 Dostmann WRG, Nickl CK, Thiel S, Tsigelny I, Frank R & Tegge WJ (1999) Delineation of selective cyclic

GMP-dependent protein kinase Ia substrate and inhibitor peptides based on combinatorial peptide libraries on paper. *Pharmacol Ther* **82**, 373–387.
31 Pinkse MW, Heck AJ, Rumpel K & Pullen F (2004) Probing noncovalent protein–ligand interactions of the cGMP-dependent protein kinase using electrospray ionization time of flight mass spectrometry. *J Am Soc Mass Spectrom* **15**, 1392–1399.
32 van den Heuvel RH & Heck AJ (2004) Native protein mass spectrometry: from intact oligomers to functional machineries. *Curr Opin Chem Biol* **8**, 519–526.
33 Heck AJ & Van Den Heuvel RH (2004) Investigation of intact protein complexes by mass spectrometry. *Mass Spectrom Rev* **23**, 368–389.
34 van Duijn E, Bakkes PJ, Heeren RM, van den Heuvel RH, van Heerikhuizen H, van der Vies SM & Heck AJ (2005) Monitoring macromolecular complexes involved in the chaperonin-assisted protein folding cycle by mass spectrometry. *Nat Methods* **2**, 371–376.
35 Wu J, Brown S, Xuong NH & Taylor SS (2004) RIalpha subunit of PKA: a cAMP-free structure reveals a hydrophobic capping mechanism for docking cAMP into site B. *Structure (Camb)* **12**, 1057–1065.
36 Su Y, Dostmann WR, Herberg FW, Durick K, Xuong NH, Ten Eyck L, Taylor SS & Varughese KI (1995) Regulatory subunit of protein kinase A: structure of deletion mutant with cAMP binding domains. *Science* **269**, 807–813.
37 Aitken A, Hemmings BA & Hofmann F (1984) Identification of the residues on cyclic GMP-dependent protein kinase that are autophophorylated in the presence of cyclic AMP and cyclic GMP. *Biochim Biophys Acta* **790**, 219–225.
38 Pinkse MW, Uitto PM, Hilhorst MJ, Ooms B & Heck AJ (2004) Selective isolation at the femtomole level of phosphopeptides from proteolytic digests using 2D-NanoLC-ESI-MS/MS and titanium oxide precolumns. *Anal Chem* **76**, 3935–3943.
39 Yuasa K, Michibata H, Omori K & Yanaka M (2000) Identification of a conserved residue responsible for the autoinhibition of cGMP-dependent protein kinase Ia and Iβ. *FEBS Lett* **466**, 175–178.
40 Tegge W, Frank R, Hofmann F & Dostmann WR (1995) Determination of cyclic nucleotide-dependent protein kinase substrate specificity by the use of peptide libraries on cellulose paper. *Biochemistry* **34**, 10569–10577.
41 Wernet W, Flockerzi V & Hofmann F (1989) The cDNA of the two isoforms of bovine cGMP-dependent protein kinase. *FEBS Lett* **251**, 191–196.
42 Keilbach A, Ruth P & Hofmann F (1992) Detection of cGMP-dependent protein kinase isozymes by specific antibodies. *FEBS Lett* **208**, 467–473.
43 Pace C, Shirley B & Thomson J (1989) In *Protein Function: a Practical Approach* (Creighton, T, ed). IRL Press, Oxford.